Some interactions of a vortex with a seamount (*)(**)

N. R. McDonald and D. C. Dunn
Department of Mathematics, University College London - Gower Street, London WC1E 6BT, UK

(ricevuto il 18 Novembre 1998; approvato il 6 Maggio 1999)

Summary. — The initial value problem for the motion of an equivalent-barotropic vortex which is initially circular and of uniform potential vorticity near a circular seamount of constant height is studied within a quasigeostrophic framework using the method of contour dynamics. Given that the radius of the vortex is equal to the deformation radius, the nature of the interaction depends on four parameters: i) the distance of the vortex from the seamount relative to the deformation radius, ii) the radius of the seamount relative to the deformation radius, iii) the ratio of the non-dimensional height of the seamount relative to the Rossby number of the vortex (or, equivalently, the vortex intensity) and iv) the sense of the vortex circulation. Contour surgery experiments are used to investigate qualitative changes in behaviour of the vortex-seamount system as these parameters are varied. Of particular note is the generation of additional vortex features by the original vortex as it sweeps fluid from the seamount. Moreover, when the original vortex is an anticyclone, dipoles are frequently formed over a wide range of parameter values, which subsequently propagate away from the seamount.

PACS 92.10.Dh – Dynamics of the deep ocean.
PACS 47.32.Cc – Vortex dynamics.
PACS 47.11 – Computational methods in fluid dynamics.
PACS 01.30.Cc – Conference proceedings.

1. – Introduction

Seamounts are common topographic features in the abyssal ocean and are sites of enhanced mixing and eddy activity over a wide range of horizontal scales (*e.g.*, Kunze and Toole [1]). It is well known that vortices may form as a result of vorticity being shed from seamounts by ambient currents. Such eddy generating mechanisms have been investigated numerically using contour dynamics by, for example, Davey *et al.* [2] and Thompson [3] and also by analytical and numerical solution of the primitive equations for a continuously stratified fluid by Huppert and Bryan [4]. Crucial to the

(*) Paper presented at the International Workshop on "Vortex Dynamics in Geophysical Flows", Castro Marina (LE), Italy, 22-26 June 1998.
(**) The authors of this paper have agreed to not receive the proofs for correction.

formation of such vortices is the presence of an anomalous potential vorticity field which, in the above cases, is provided by the topography of the seamount. Seamounts are only one example of topographic features that may give rise to vortex generation when currents flow over them. For instance, Cherubin *et al.* [5] discuss the generation of vortices by flow of a coastal jet over a canyon.

The focus of the present work is the interaction of vortices, rather than currents, with seamounts. Such interactions are certainly possibilities in the ocean, since vortices may, by their ability to self-advect owing to, say, the β-effect, or by their advection by larger-scale currents, eventually encounter a seamount. The present work does not address the issue of how the vortex came to be situated close to the seamount but instead focuses on the initial value problem of suddenly initiating a vortex flow near the seamount. The large localised velocities associated with the vortex may then cause fluid in the vicinity of the seamount to cross isobaths which, in turn, generates vorticity by the stretching mechanism. The subsequent evolution of the coupled system of shed vorticity and the original vortex depends on the strength, sense of circulation and the location of the vortex as well as the height and radius of the seamount. This makes the problem of vortex-seamount interaction much richer and complex than, say, the interaction of a uniform current with a seamount.

To illustrate some of the possibilities for the types of interaction for the vortex-seamount problem, quasigeostrophic dynamics for a single active layer of fluid whose surface may deform (*i.e.* equivalent-barotropic) are assumed. Quasigeostrophy requires that both the Rossby number of the flow and the height of the seamount compared to the average layer depth are small parameters. In the special case of piecewise constant distributions of potential vorticity, accurate long-time integration of the non-linear equation of motion is enabled by the method of contour surgery (Dritschel [6]). In order to use this method here it is assumed that the vortex is a uniform patch of potential vorticity and the seamount is a circular cylinder of uniform height. Even with these simplifications and assuming the vortex is the size of the deformation radius, there are four parameters that determine the flow evolution (see sect. **2** for a discussion of these parameters). Rather than a thorough, quantitative, investigation of the entire parameter space, the aim here is provide some examples of the different types of interactions that may take place. These examples will be illustrated qualitatively by plotting the evolution of the contours describing the vortex and the potential vorticity anomaly initially overlying the seamount.

2. – Governing equations and parameters

The fluid layer has a typical depth H, reduced gravity g' and contains a circular seamount with constant height ΔH and radius a. Let f be the Coriolis parameter. In the following it shall be assumed, as is typical for many ocean vortices, that the vortex, initially circular, has a radius equal to that of the deformation radius. Choosing the deformation radius $\sqrt{g' H}/f$ as the lengthscale L, the non-dimensional quasigeostrophic potential vorticity q, a conserved quantity, is

$$q = \nabla^2 \psi - \psi + Sh \,. \tag{1}$$

Here ψ is the streamfunction, $h(x, y)$ is the non-dimensional height of the topography and $S = \delta/\mathrm{Ro}$, where $\delta = \Delta H/H$ and $\mathrm{Ro} = U/fL$ is the Rossby number and δ, $\mathrm{Ro} \ll 1$ (see also Davey *et al.* [2]). The streamfunction has been non-dimensionalised using the scale

Ro fL^2. In calculating Ro here, the choice of typical velocity U is the swirl velocity at the periphery of the vortex, *i.e.* at a lengthscale equal to that of the deformation radius. The dimensional timescale for the motion is the advective time $f^{-1}\mathrm{Ro}^{-1} = L/U$. Alternatively, S can be written as

$$S = \frac{\delta}{\mathrm{Ro}} = \frac{L/U}{(H/\Delta H)\, f^{-1}}, \tag{2}$$

which is the ratio of the advective time to the topographic vortex stretching time and sometimes known as the vortex intensity (McDonald [7]). The seamount is centred at the origin, *i.e.*

$$h(x, y) = \begin{cases} 1, & r \leqslant a, \\ 0, & r > a, \end{cases} \tag{3}$$

where $r^2 = x^2 + y^2$.

For small S, the effect of topography is weak (or the vortex very strong) and the fluid initially lying over the seamount acts, to leading order, like a passive tracer. In this limit and when the topography was an infinitely long escarpment, McDonald [7] was able to calculate the response of a point vortex to first order in S. On the other hand, for large S, the effect of topography is dominant (or the vortex very weak) and again for topography in the form of an infinitely long escarpment, Dunn [8] has shown that the escarpment acts (at least for times large compared to the topographic vortex stretching time) like a wall, *i.e.* it inhibits cross-isobath motion and the vortex moves as though it were being advected by its image in the escarpment. Although it may be possible to perform a similar asymptotic analysis for both large and small S for topography in the form of a circular seamount, attention here shall be on the highly non-linear case when the effect of topography and advection by the vortex are comparable, *i.e.* values of S which are of order unity. Such a parameter regime is inaccessible via asymptotic methods but is suitable for investigation using the numerical method of contour surgery (Dritschel [6]).

Let T denote the fixed topographic contour defined by the boundary of the seamount $r = a$, A the material contour that initially coincides with T and V the material contour which encloses the uniform patch of relative vorticity of the vortex. Due to the scaling this vorticity is either $+1$ for a cyclone or -1 for an anticyclone. Initially,

$$q = \begin{cases} S, & \text{inside A}, \\ \pm 1, & \text{inside V}, \\ 0, & \text{elsewhere}. \end{cases} \tag{4}$$

Equations (1) and (4) imply for subsequent times (see fig. 1)

$$\nabla^2 \psi - \psi = \begin{cases} -S, & \text{inside T and outside A (region (i))}, \\ S, & \text{inside A and outside T (region (iii))}, \\ \pm 1, & \text{inside V (region (iv))}, \\ 0, & \text{elsewhere (regions (ii) and (v))}. \end{cases} \tag{5}$$

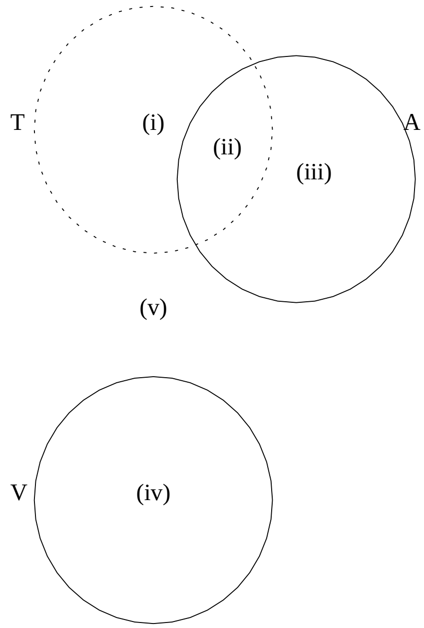

Fig. 1. – The various regions of the flow. The topographic, advected and vortex contours are denoted T, A and V, respectively. Region (i) consists of fluid that has moved on to the seamount, acquiring relative vorticity $-S$, (iii) consists of fluid that has moved off the seamount acquiring relative vorticity $+S$, (iv) is the constant relative vorticity fluid of the vortex and the regions (ii) and (v) consist of ambient fluid with zero relative vorticity.

The velocity field is determined by inversion of (5) by Green's theorem, which gives for the point (x, y)

$$(u, v) = (u_{\mathrm{T}}, v_{\mathrm{T}}) - \frac{S}{2\pi}\int_A K_0(r_0)(\mathrm{d}x_0, \mathrm{d}y_0) \mp \frac{1}{2\pi}\int_V K_0(r_0)(\mathrm{d}x_0, \mathrm{d}y_0), \tag{6}$$

where $r_0^2 = (x - x_0)^2 + (y - y_0)^2$. The contribution $(u_{\mathrm{T}}, v_{\mathrm{T}})$ due to the fixed topographic contour can be calculated explicitly (see Davey *et al.* [2]) by solving the zero potential vorticity problem for the associated streamfunction ψ_{T}, for a right circular cylinder of radius a and unit height, *i.e.* solving

$$\nabla^2\psi_{\mathrm{T}} - \psi_{\mathrm{T}} = \begin{cases} -S, & r \leqslant a, \\ 0, & r > a. \end{cases} \tag{7}$$

Demanding that ψ_{T}, and its radial derivative, be continuous at $r = a$, gives

$$\psi_{\mathrm{T}} = \begin{cases} S - aSK_1(a)\, I_0(r), & r \leqslant a, \\ aSI_1(a)\, K_0(r), & r > a. \end{cases} \tag{8}$$

The velocity components due to the seamount are then obtained from (8) by $u_{\mathrm{T}} = -\psi_{\mathrm{T}_y}$ and $v_{\mathrm{T}} = \psi_{\mathrm{T}_x}$. The contour nodes are advected using a fourth-order Runge-Kutta scheme, and the nodes are redistributed at each time step through a non-local node-density function. Surgery is performed at a prescribed scale. See Dritschel [6] for full details of the algorithm.

The accuracy of the algorithm was tested by successfully reproducing the results of Davey *et al.* [2] for the sudden initiation of a uniform stream over a seamount, and the appropriate vortex-merger results of Waugh [8] (*i.e.* his quasigeostrophic shallow water vortex-merger results) with the background potential vorticity field contribution due to the topography switched off.

In addition to S, there are three other parameters appropriate to this problem: i) the size of the seamount relative to the vortex (or deformation) radius, ii) the initial distance of the vortex from the seamount and iii) the sense of vortex circulation, *i.e.* whether it is a cyclone or an anticyclone. Note that iii) is equivalent to changing the sign of S. That is, a cyclone near a seamount will evolve in the same way as an anticyclone near a hollow. The effect of changing these parameters are investigated in the next sections.

3. – The effect of varying the distance of the vortex from the seamount

The first experiment consists of an anticyclonic vortex of unit radius (hereafter referred to as the original vortex) located near a seamount also of unit radius such that the closest distance between the vortex and the seamount peripheries is 0.1 and $S = 1$. Figure 2a) shows the evolution of the vortex at intervals of ten time units. The boundary of the topography ($r = 1$ in this example) is shown as a dashed circle in each frame. At $t = 10$ the clockwise swirl velocity associated with the anticyclonic vortex has swept some of the fluid off the seamount. This fluid undergoes vortex stretching, producing cyclonic vorticity of equal magnitude (since $S = 1$) to the vorticity of the original vortex. The anticlockwise circulation associated with this cyclonic vortex comprising of fluid initially overlying the seamount (hereafter referred to as the seamount fluid vortex) has, in turn, begun to deform the original vortex. The dipolar nature of the original vortex and the vortex comprising of fluid originally from the seamount, cause the seamount fluid vortex to propagate some distance from the seamount up to $t = 20$. After $t = 20$ the dipolar propagation mechanism begins to weaken owing to the continued deformation of the original vortex. The unequal influence of the original vortex and the seamount fluid vortex on each other due to their unequal areas, causes the dipole to follow a curved path back toward the seamount. This curved path continues at $t = 40$ and $t = 50$, whereupon the remainder of the original vortex begins to exert its influence on the seamount fluid vortex and a larger dipole is just beginning to form which again will propagate away from the seamount. Note that some of the fluid originally located over the seamount remains trapped by the seamount.

Figure 2b) depicts the same experiment as shown in fig. 2a) except that the distance between the boundaries of the vortex and seamount has increased to 1. Owing to the pseudo-exponential decay of the modified Bessel Green's function in (6) for large distances (*i.e.* $K_0(r) \sim e^{-r}/\sqrt{r}$ as $r \rightarrow \infty$), it is expected that the interaction of the vortex and seamount be less strongly coupled compared to the previous experiment. Indeed this is evident with considerably less fluid being swept off the seamount at, say, $t = 20$ compared to fig. 2a). Nonetheless, the evolution displays similar characteristics to the experiment shown in fig. 2a). In particular, the cyclonic vorticity of the fluid

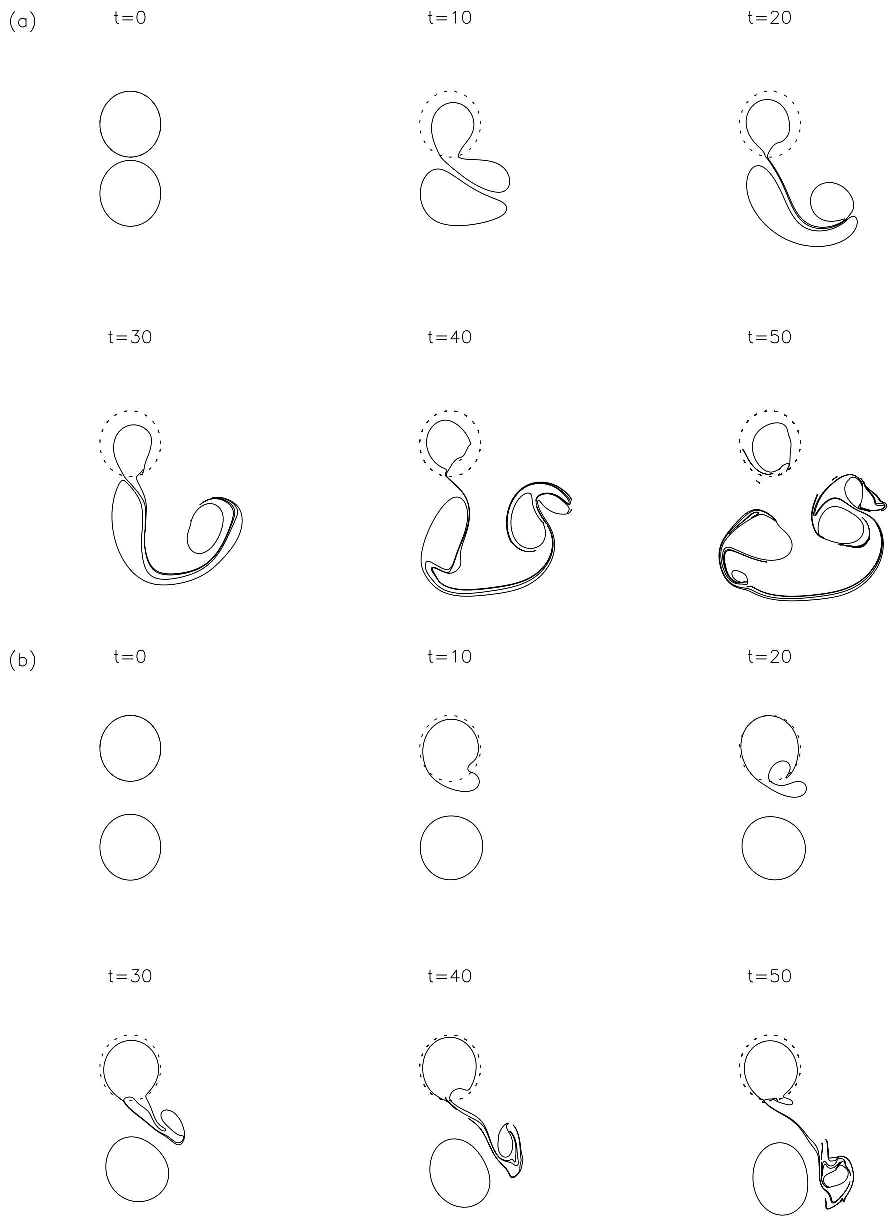

Fig. 2. – Evolution of vortex-seamount system for an anticyclone with $S = 1$ and $\alpha = 1$. The distance between the peripheries of the vortex and seamount is a) 0.1 and b) 1. The topographic contour representing the seamount is shown by a dashed circle.

originating from the seamount couples with the vortex to form a dipole which propagates away from the seamount. Because, in this case, the original vortex is much larger than the seamount fluid vortex the dipole-effect is again uneven but now the path curves to a lesser degree, and in the opposite sense, to that shown in fig. 2a). Also, because the area of fluid swept from the seamount is relatively small, and further away, the deformation of the original vortex is smaller in this case.

Not surprisingly, the trend when increasing the separation distance between the vortex and seamount is for the amount of fluid shed by the seamount to decrease, and consequently for the deformation and displacement of the original vortex to decrease. For example, when the distance between the vortex and seamount boundaries increases to 1.5 (not shown), there is no discernible vortex formed from fluid shed from the seamount by $t = 50$ and the original vortex effectively remains undisturbed.

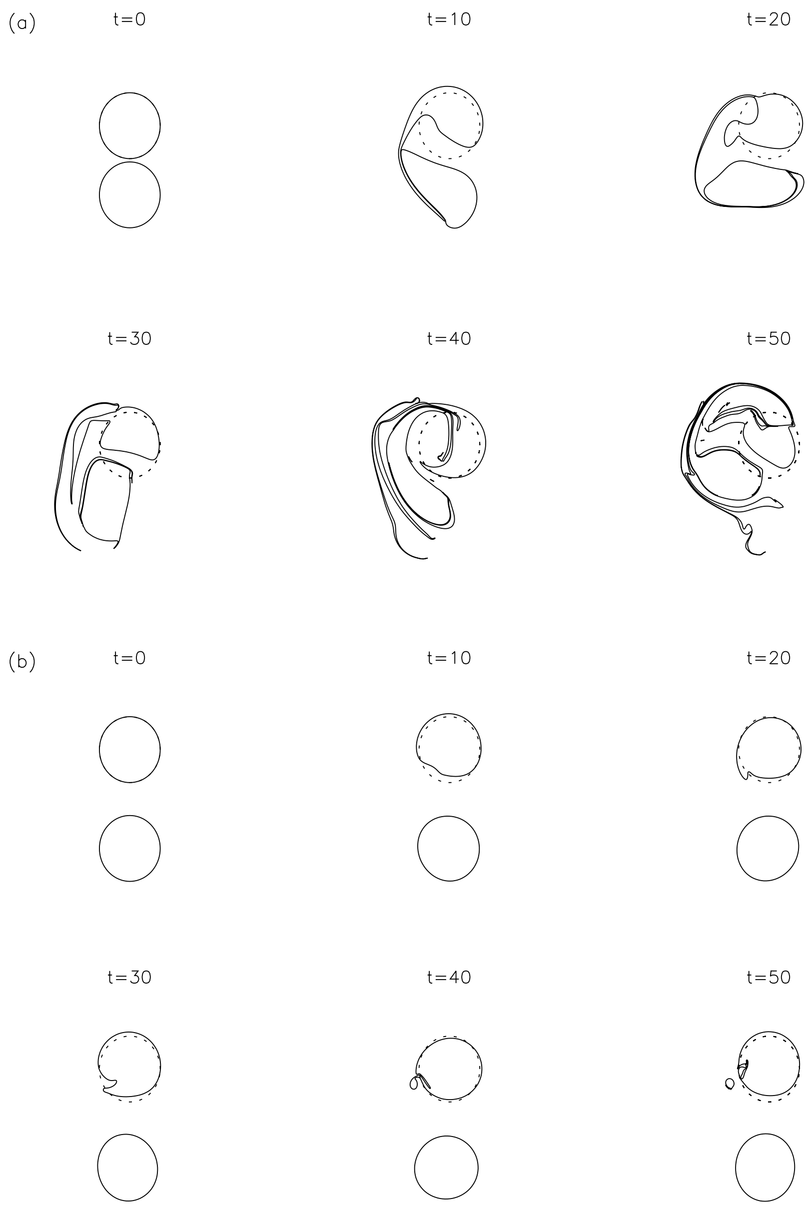

Fig. 3. – As in fig. 2, but for a cyclone.

4. – Reversing the sense of vortex circulation

The previous two experiments were repeated using cyclones instead of anticyclones and the results are shown in fig. 3a), b). The evolution is significantly different than for the anticyclone case. In fig. 3a) the vortex tends to slowly strip the seamount of its fluid. Once the fluid has been forced off the seamount by the vortex it acquires cyclonic vorticity of equal magnitude to the vortex. The problem then becomes very much like the vortex merger problem (for vortices with identical vorticity/potential vorticity) described by, for example, Waugh [9], Dritschel and Waugh [10] and Polvani *et al.* [11] except for the addition of the background potential vorticity field due to the presence of the seamount. In particular, the small area of fluid shed from the seamount is stretched and wrapped around the primary vortex before merger (cf. the merger results of [10] for unequal sized vortices with the same vorticity). In fact, though it is not clear in fig. 3a), the vortex-seamount system has momentarily merged into a single contour at $t = 20$. This process is seen to repeat itself, with another filament been shed and wrapped around the vortex, for example, at time $t = 30$. The loss of fluid from the seamount implies that a residual clockwise circulation develops around the seamount due to vortex compression of the fluid, originally from deep water moving onto the seamount to replace the fluid shed from there (this circulation is also evident in the anticyclone experiments shown in fig. 2a), b)). This circulation deforms the original vortex as seen at $t = 10$, and is also responsible for rotation of the original vortex between $t = 20$ and $t = 30$ and the general translation of the vortex observed up to $t = 50$. In contrast to the anticyclone case, the original cyclone remains trapped near the vortex.

Figure 3b) shows that the influence of the vortex on the fluid overlying the seamount is considerably reduced compared to that shown in fig. 3a). Eventually by $t = 50$ a cyclone comprising of fluid originally from the seamount with small radius has formed. There is no discernible deformation of the primary vortex. Note that the vortex produced here is much smaller than the anticyclone experiment with the same parameters (fig. 2b). The reason for this is that the initial advection of the contour encircling the seamount toward deeper water, due to the original vortex, moves away from the vortex as it cycles clockwise around the seamount, *i.e.* with shallow water on its right. For the case of the anticyclone (fig. 2b) the initial disturbance moves toward the original vortex and so grows larger, before forming a distinct vortex.

5. – Use of point vortices

The relatively small deformation of the vortex shown in fig. 2b) up to $t = 50$ suggests that replacing the vortex patch by a point vortex may produce similar results for the evolution of the contour surrounding the seamount. To test this hypothesis the vortex patch was replaced by a point vortex with identical structure to the vortex patch for $r > 1$ and run for the same parameters as the experiment shown in fig. 2b). The results are displayed in fig. 4a), where the location of the point vortex is marked by a cross. Comparison with fig. 2b) indeed shows that the evolution of the seamount contour is very similar in both cases. In contrast, the deformation of the vortex in fig. 2a) suggests that it would be poorly modelled by a point vortex. To demonstrate this, fig. 4b) shows the evolution of the seamount contour for an experiment equivalent to that shown in fig. 2a) but with a point vortex replacing the vortex patch. Comparison shows that the

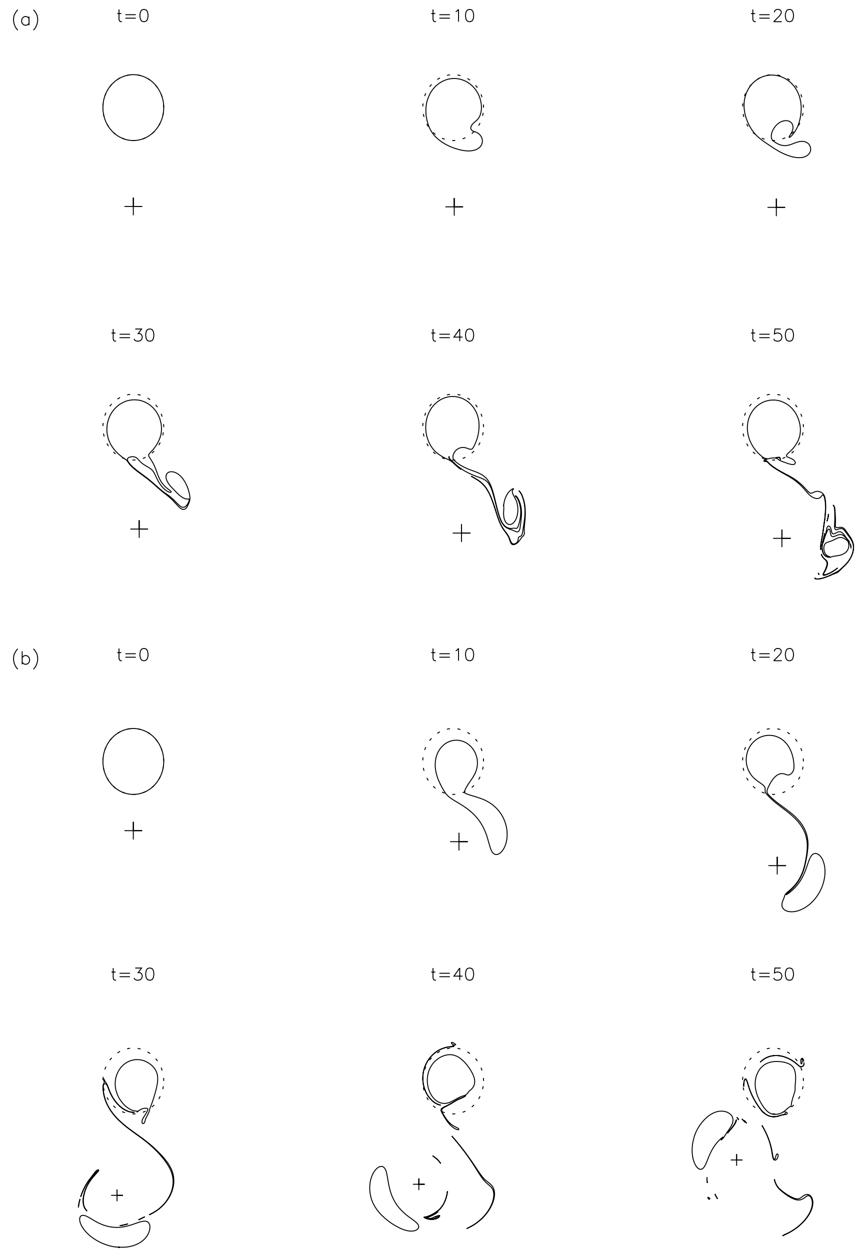

Fig. 4. – Evolution of a point vortex-seamount system for an anticyclone with $S = 1$ and $a = 1$. The location of the point vortex is indicated by a +. The distance between the peripheries of the vortex and seamount is a) 1.0 and b) 0.1.

evolution of the seamount is markedly different owing to the inability of the point vortex to deform. A general conclusion is that point vortex models of vortex-topography interaction are useful only when the deformation of an equivalent vortex patch is likely to be small. For the case of seamount topography here, this is likely, at least for times up to $t = 50$, when the initial distance of the peripheries of the vortex and seamount is at least a deformation radius.

6. – The effect of varying the size of the seamount

In the following experiments an anticyclone, with $S = 1$, is located such that the periphery of the vortex is 0.1 from the edge of the seamount, *i.e.* the same as in fig. 2a). Experiments were performed (not shown) increasing the seamount radius from unity and the evolution of the system was found to be similar to that shown in fig. 2a). That is, a dipole structure formed which propagates away from the seamount. To demonstrate this, the evolution for an infinitely long escarpment (which can be thought of as a seamount with infinite radius of curvature) is shown in fig. 5a). Note that in this case the contribution due to the topography ψ_T is calculated numerically owing to problems of representing an infinitely long escarpment by one of finite length in the contour dynamics code. Comparison with fig. 2a) demonstrates the similarity, although there are some differences. In particular, in fig. 5a) the original vortex remains more coherent in comparison to fig. 2a). This is due to the relatively small residual clockwise circulation set-up about the seamount (or escarpment in this case) formed when fluid from deeper surrounds replaces fluid swept from the escarpment and undergoes vortex compression (*i.e.* region (i) of fig. 1—see later discussion of this section). The reduced circulation results in less stretching of the original vortex.

On the other hand, for seamounts with radius less than unity, the evolution of the system is significantly different. The effect of the residual clockwise circulation is particularly evident in fig. 5b), which is for a seamount of radius 0.5. Here, by $t = 10$ virtually all the fluid has moved off the seamount. The clockwise circulation about the seamount and the anticlockwise circulation of the shed vortex cause severe distortion of the primary vortex. By $t = 50$ roughly half of the original vortex is trapped by the seamount and the other half combines with the seamount shed vortex to form a dipole propagating away from the seamount.

In summary, for seamounts of smaller radius than the vortex the evolution is quite different than for seamounts of the same, or larger, radius than the vortex. For small seamounts the vortex has the ability to sweep all of the fluid from the seamount, *i.e.* a relatively large region (i). The resulting residual clockwise circulation then traps some of the original vortex near the seamount. This effect is not observed for seamount with radius bigger than unity, since the percentage of fluid lost from the seamount (region (i)) is relatively small and therefore the residual circulation about the seamount is correspondingly small.

7. – The effect of varying S

The effect of varying the parameter S, the ratio of the non-dimensional height of the seamount to the Rossby number of the vortex is investigated. Figure 6a) shows the evolution of an anticyclone with $S = 1/2$ with the other conditions being identical to fig. 2a). Again there is a tendency for a dipole to form, since fluid initially overlying the seamount acquires cyclonic relative vorticity when it moves from the seamount into deeper water. However, compared to that in fig. 2a), the relative vorticity so produced is half the magnitude of the vorticity of the primary vortex. Note also that since S is smaller here than in fig. 2a), the more passive it is and so more is dragged from the seamount by the original vortex. The dipole, owing to the unequal magnitude of vorticities, follows a curved path, this time curving in the opposite sense to that in fig. 2a) since the magnitude of the original vortex vorticity is twice that of the seamount fluid vortex.

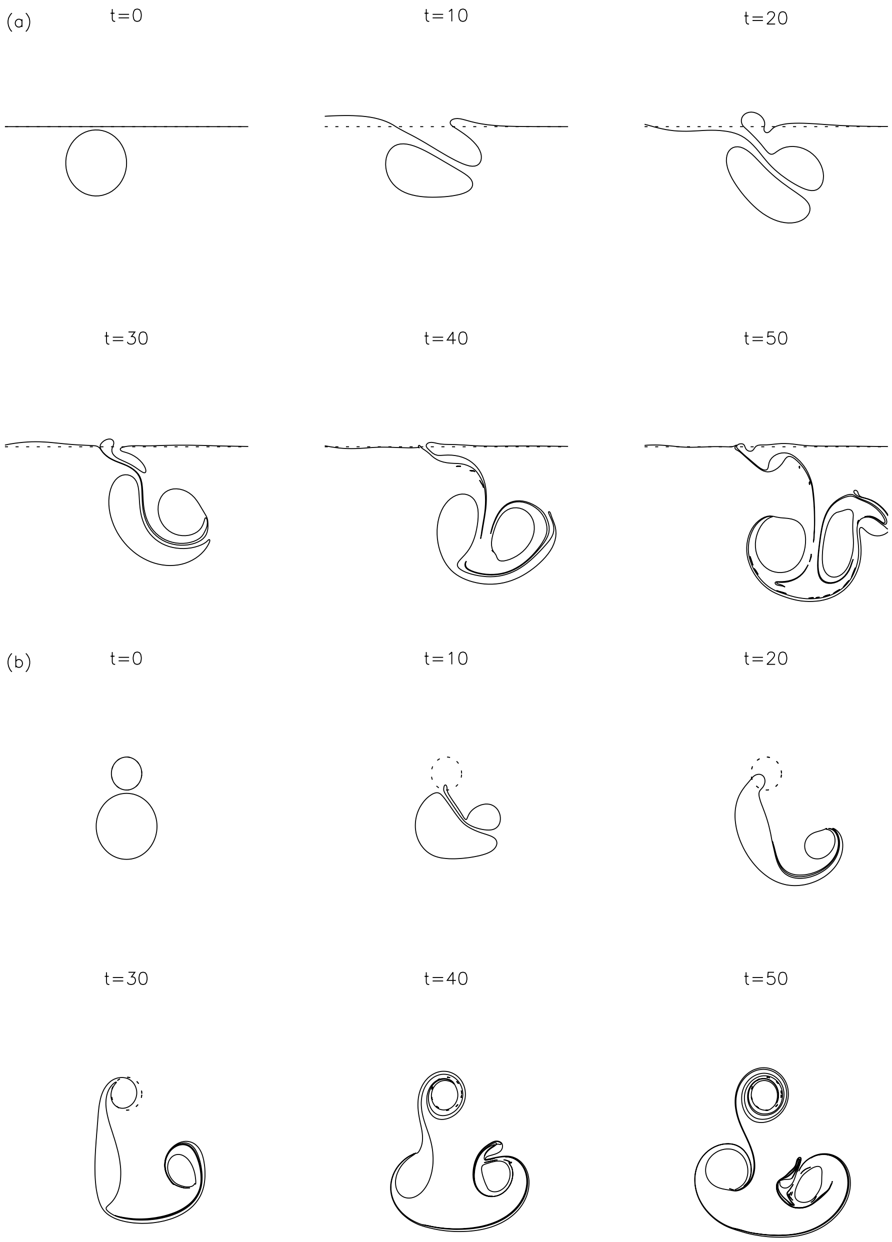

Fig. 5. – Evolution of a vortex-topography system for an anticyclone with $S = 1$ and the distance between the periphery of the vortex and the topography is 0.1. a) Infinitely long escarpment, b) seamount of radius $a = 0.5$.

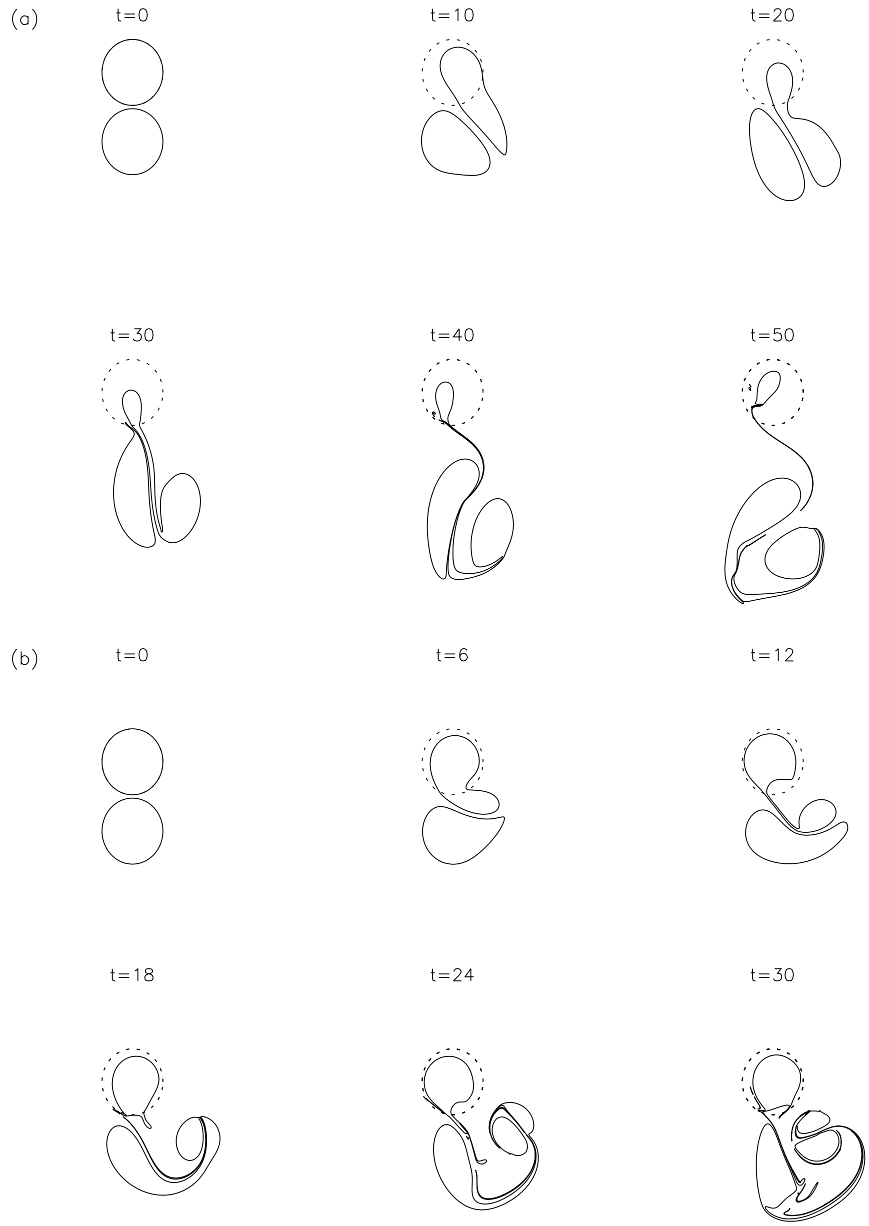

Fig. 6. – Evolution of a vortex-seamount system for an anticyclone with $a = 1$ and the distance between the peripheries of the vortex and the seamount is 0.1. a) $S = 0.5$ and b) $S = 1.5$.

An identical experiment was performed with $S = 1.5$ and the results are shown in fig. 6b). Note now the plots are intervals of 6 time units since the evolution, though similar to that in fig. 2a), is now more rapid. The dipole evident at $t = 24$ and $t = 30$ follows a tighter curve than the corresponding dipole in fig. 2a). This is because the vorticity in the seamount fluid vortex has a magnitude 1.5 times that of the original vortex and so the dipole propagation mechanism is not symmetric not only in terms of area but also of vorticity.

8. – Conclusions

The interaction of a vortex of constant potential vorticity with a circular seamount of constant height has been explored in a quasigeostrophic framework using the method of contour surgery. For a vortex whose radius is that of the deformation radius, the evolution of the system depends on four parameters: i) the distance between the vortex and seamount; ii) the parameter S, the ratio of the non-dimensional fractional height of the seamount to the Rossby number of the vortex; iii) the sign of the vortex circulation and iv) the radius of the seamount. No attempt was made to systematically explore the multi-dimensional parameter space, the emphasis instead was in illustrating some of the possible interactions that may take place. In particular, when the vortex is sufficiently strong, or the topography small (*i.e.* small S) and/or the vortex sufficiently close to the seamount (*i.e.* their closest points less than about a deformation radius) a significant amount of fluid is swept off the escarpment by the vortex. Subsequent vortex stretching leads to the formation of a cyclonic vortex. In the case when the original vortex was an anticyclone, the cyclonic vortex comprising of seamount fluid pairs up with the original vortex to form a dipole. The dipolar propagation mechanism causes the pair to travel initially away from the seamount in a path which curves in a manner dependent on the parameters of the system. The formation of a dipole is found to be a robust feature and occurs over wide region of the parameter space. Such dipole formation has been observed in experiments on monopolar vortices impinging on shallow shelves (van Heijst [12]).

* * *

NRM is grateful to the Royal Society for providing funds to attend the Castro conference. The work of DCD was supported by a NERC studentship.

REFERENCES

[1] KUNZE E. and TOOLE J. M., *Tidally driven vorticity, diurnal shear, and turbulence atop Fieberling Seamount*, *J. Phys. Ocean.*, **27** (1997) 2663-2693.

[2] DAVEY M. K., HURST R. G. A. and JOHNSON E. R., *Topographic eddies in multilayer flow*, *Dyn. Atmos. Oceans*, **18** (1993) 1-27.

[3] THOMPSON L., *Two-layer quasigeostrophic flow over finite isolated topography*, *J. Phys. Ocean.*, **23** (1993) 1297-1314.

[4] HUPPERT H. E. and BRYAN K., *Topographically generated eddies*, *Deep-Sea Res.*, **23** (1976) 655-679.

[5] CHERUBIN L. M., CARTON X. J. and DRITSCHEL D. G., *Vortex expulsion by a zonal coastal jet on a transverse canyon*, *ESIAM: Proc.*, **1** (1996) 481-501.

[6] DRITSCHEL D. G., *Contour surgery: a topological reconnection scheme for extended integrations using contour dynamics*, *J. Comput. Phys.*, **77** (1988) 240-266.

[7] McDonald N. R., *The motion of an intense vortex near topography*, *J. Fluid Mech.*, **367** (1998) 359-377.
[8] Dunn D. C., PhD Thesis, University College, London (1998).
[9] Waugh D., *The efficiency of symmetric vortex merger*, *Phys. Fluids A*, **4** (1992) 1745-1758.
[10] Dritschel D. G. and Waugh D., *Quantification of the inelastic interaction of unequal vortices in two-dimensional vortex dynamics*, *Phys. Fluids A*, **4** (1992) 1737-1744.
[11] Polvani L. M., Zabusky N. J. and Flierl G. R., *Two-layer geostrophic vortex dynamics. Part 1: upper layer V-states and merger*, *J. Fluid Mech.*, **205** (1989) 215-242.
[12] Zavala Sansón L., van Heijst G. J. F. and Doorschoot J. J. J., this issue, p. 790.